Pergamon

Journal of Structural Geology, Vol. 18, No. 7, pp. 863 to 869, 1996

0191-8141/96 $15.00+0.00

PII: S0191-8141(96)00013-2

Composite magnetic fabrics from S-C mylonites

AITOR ARANGUREN, JULIA CUEVAS and JOSE M. TUBÍA

Departamento de Geodinámica, Universidad del País Vasco, Apdo. 644, Bilbao 48080, Spain

(*Received* 4 *July* 1995; *accepted in revised form* 24 *January* 1996)

Abstract—Magnetic anisotropy data are presented for samples of S-C mylonites from a shear zone developed in the Veiga granodiorite, a late-kinematic pluton located in the northern part of the Iberian Variscan belt (Spain). The magnetic susceptibility is geometrically represented by an ellipsoid whose principal axes, $K_{max} \geq K_{int} \geq K_{min}$, often show a one-to-one correlation with the principal directions—X,Y and Z—of finite strain. We report an exception to this rule, since our results reflect composite magnetic fabrics arising from the contribution of both the C- and S-structures. The magnetic foliation, defined as the plane normal to K_{min}, shows an intermediate orientation between the C- and S-planes, and rotates towards the orientation of the C-planes as finite strain increases. The magnetic lineation, parallel to K_{max}, and the stretching lineation present a similar trend, but different values of plunge. Copyright © 1996 Elsevier Science Ltd

INTRODUCTION

After Graham's (Graham 1954) pioneering paper on the potential of the Anisotropy of Magnetic Susceptibility (AMS) for structural analysis, many efforts have been made to decipher the relationship between the magnetic fabrics and the structural record of tectonites (see Tarling & Hrouda 1993 for a recent compilation of different AMS applications). Such interest is amply justified because the magnetic susceptibility is a petrophysical property which can be expressed by a symmetrical tensor of second order and geometrically represented as an ellipsoid (Jelinek 1981) whose principal axes, $K_{max} \geq K_{int} \geq K_{min}$, often show a one-to-one correlation with the main directions—X, Y and Z—of finite strain (Borradaile 1991, Hrouda 1993). This statement is supported by many studies, dealing with: (1) empirical results from deformed rocks, of sedimentary (Kligfield *et al.* 1981, Rochette & Vialon 1984), metamorphic (Borradaile 1991) and igneous (Van der Voo & Klootwijk 1972, Jover *et al.* 1989) origins, (2) experimental tests showing the variation of the AMS in analogue materials submitted to deformation (Borradaile & Alford 1988), and (3) numerical models which reproduce the magnetic fabric of rocks (Benn 1994). However, magnetic fabric ellipsoid axes may not correlate with the finite strain axes as a result of structural evolutions leading to domainal fabrics (Hrouda 1991) or, alternatively, due to the presence of minerals with an inverse magnetic fabric, such as tourmaline (Rochette *et al.* 1994) or single-domain magnetite crystals (Potter & Stephenson 1988). Consequently, any accurate petrofabric interpretation of AMS data requires complementary data on the structural and microstructural features of the measured samples and on the identification of the magnetic carriers.

This work is mainly concerned with the structural significance of AMS-directional data in S-C mylonites showing two well defined sets of planar-linear structures intersecting at variable angles with a uniform sense of obliquity. Our results represent an exception to the rule of coaxiality between magnetic and finite strain ellipsoids, since our samples provide composite magnetic fabrics which clearly depart from the orientations of both the S-plane and the C-plane. The studied samples come from the Chandoiro Fault (NW Spain), a ductile normal-shear zone up to 1,200 m thick, developed along the western border of the Veiga granodiorite (Iglesias & Varea 1982). The Veiga granodiorite is a late Hercynian, syn-kinematic pluton which intrudes into the Precambrian and Palaeozoic metamorphic rocks of the Iberian Variscan belt (Fig. 1). Determinations of the AMS were performed with a KLY-2 magnetic susceptibility bridge operating at a low magnetic field ($\pm 4 \times 10^{-4}$ T and 920 Hz) with a resolution better than 5×10^{-8} SI units, and manufactured by Geofyzika (Brno, Czech Republic).

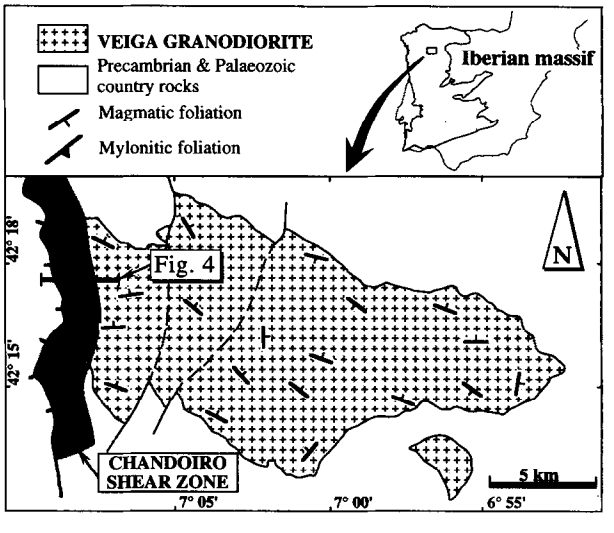

Fig. 1. Location of the Chandoiro Fault along the western contact of the Veiga granodiorite. The insert shows the location of the Veiga granodiorite within the Hercynian belt of Portugal and Spain.

STRUCTURAL VARIATION ACROSS THE CHANDOIRO FAULT

Solid state strain distribution in the Veiga granodiorite is heterogeneous and largely concentrated in the Chandoiro Fault. This shear zone strikesN–S and dips 40–70° to the west (Fig. 1). Outside the shear zone (d > 1,200 m) the granodiorite shows no evidence of solid-state deformation. These rocks display a magmatic foliation defined by aligned and euhedral K-feldspar megacrysts in a coarse-grained matrix rich in equiaxial and strain-free grains of quartz (Fig. 2A). Many granodiorite samples from the Chandoiro Fault are mylonitic rocks displaying composite planar fabrics formed by S-C structures. C-structures are spaced planes rich in biotite which show a mean orientation coincident with that of the shear zone boundary. Between these spaced C-planes there is a well-developed penetrative foliation, the S-planes, that dips more shallowly than C (Fig. 2B). The S-C structure changes progressively across the shear zone. With increasing strain, the angle between the S and C planes decreases and the presence of C planes increases. Following Berthé *et al.* (1979) and Lister & Snoke (1984), C-planes can be interpreted as forming subparallel to the shear plane whereas S-surfaces correspond to the XY plane of the finite strain ellipsoid. In the most highly strained zones, close to the contact with the country rocks (d < 50 m), the two sets of planar structures become subparallel and a new set of shear bands develop locally. These shear bands, designated as C′-planes by Iglesias & Choukroune (1980), form at a low angle, ≈ 30°, to the dominant S + C foliation. At increasing distance from the contact (50 to 800 m), the angle between the C- and S-planes increases progressively from 0 to 45° and the width of S-domains between adjacent C-planes increases up to 2 cm. Finally, in the less strained zones solid-state deformation is only recorded by some isolated and very weakly developed shear bands in otherwise apparently isotropic granodiorites (Fig. 2C). Prominent stretching lineations are developed on both the C and S-planes (Fig. 2D). Defined by the preferred orientation of stretched quartz and biotite aggregates, this lineation trends E–W and plunges 30–60° to the west.

The S-domains consist essentially of biotite, oligoclase, K-feldspar and quartz, with minor amounts of secondary muscovite. The content in biotite varies between 10.5 and 13.6%. Allanite, ilmenite and zircon are found as accessory minerals. The C-domains show a noticeable enrichment in biotite (30 to 62%) (Fig. 3A). The instability of biotite during mylonitization led to the development of small grains of oxides that are mainly concentrated along the (001)-cleavage and grain boundary of biotites belonging to the C-domains (Fig. 3B).

AMS-DIRECTIONAL DATA

The effect of increasing finite strain on AMS is shown in Fig. 4, with a regular sampling of 48 stations

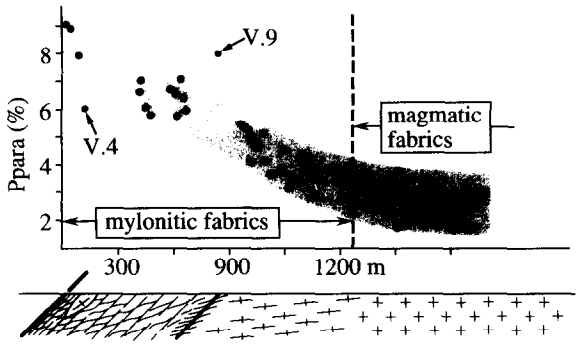

Fig. 4. Variation of the magnetic anisotropy, P_{para} %, (48 sampling sites) across the Chandoiro Fault. Samples V.4 and V.9, departing from the trend outlined by the remaining samples, reflect the heterogeneity of strain across the shear zone. The location of the studied section of the Chandoiro Fault is indicated in Fig. 1.

distributed along a cross-section perpendicular to the Chandoiro Fault. In order to avoid local disturbances of the magnetic properties, four oriented cores per station were taken using the same procedure as for palaeomagnetic studies. As previously stated, since some minerals may produce inverse magnetic fabrics where K_{max} is the pole to planar structures of the measured rocks (Potter & Stephenson 1988, Rochette *et al.* 1994), any petrofabric interpretation of AMS-data requires the identification of the magnetic carriers. Isothermal remanent magnetization data recently obtained in the Veiga granodiorite (Román-Berdiel *et al.*, in press) have shown that the contribution of ferromagnetic minerals is lower than 0.05×10^{-5} SI, with an average value of 0.03% of the total susceptibility. Therefore, the magnetic susceptibility of our samples, which ranges between 5.5 × and 36.7×10^{-5} SI, is of dominant paramagnetic origin and mainly due to the widespread presence of biotite crystals.

The total anisotropy of the magnetic susceptibility is taken as:

$$P_{\text{para}}\% = 100 \times [((K_1 - D)/(K_3 - D)) - 1],$$

where $D = -1.4 \times 10^{-5}$ SI is the contribution of diamagnetic minerals, mainly quartz and feldspar, to the overall magnetic susceptibility of the sample (Hrouda 1986, Rochette 1987). The introduction of D in the formula is justified because precise anisotropy determinations are required to study the strain gradient, and in these weakly susceptible rocks the contribution of diamagnetic minerals tends to increase the anisotropy. Outside the shear zone, P_{para} % values range between 1.7 and 3.9. Such low values are usually found in paramagnetic granitic rocks that crystallized under (solid-state) strain-free conditions (Jover *et al.* 1989, Bouchez *et al.* 1990). With increasing strain, the magnetic anisotropy shows a progressive non-linear increase up to P_{para} % = 9.02 near the contact with the country rocks. Samples V.4 and V.9, exhibiting unusually low and high P-values, respectively, depart from the trend outlined in Fig. 4. They probably reflect the heterogeneity of strain across the shear zone, since V.4 comes from a lens-shaped body of coarse-grained protomylonites preserved

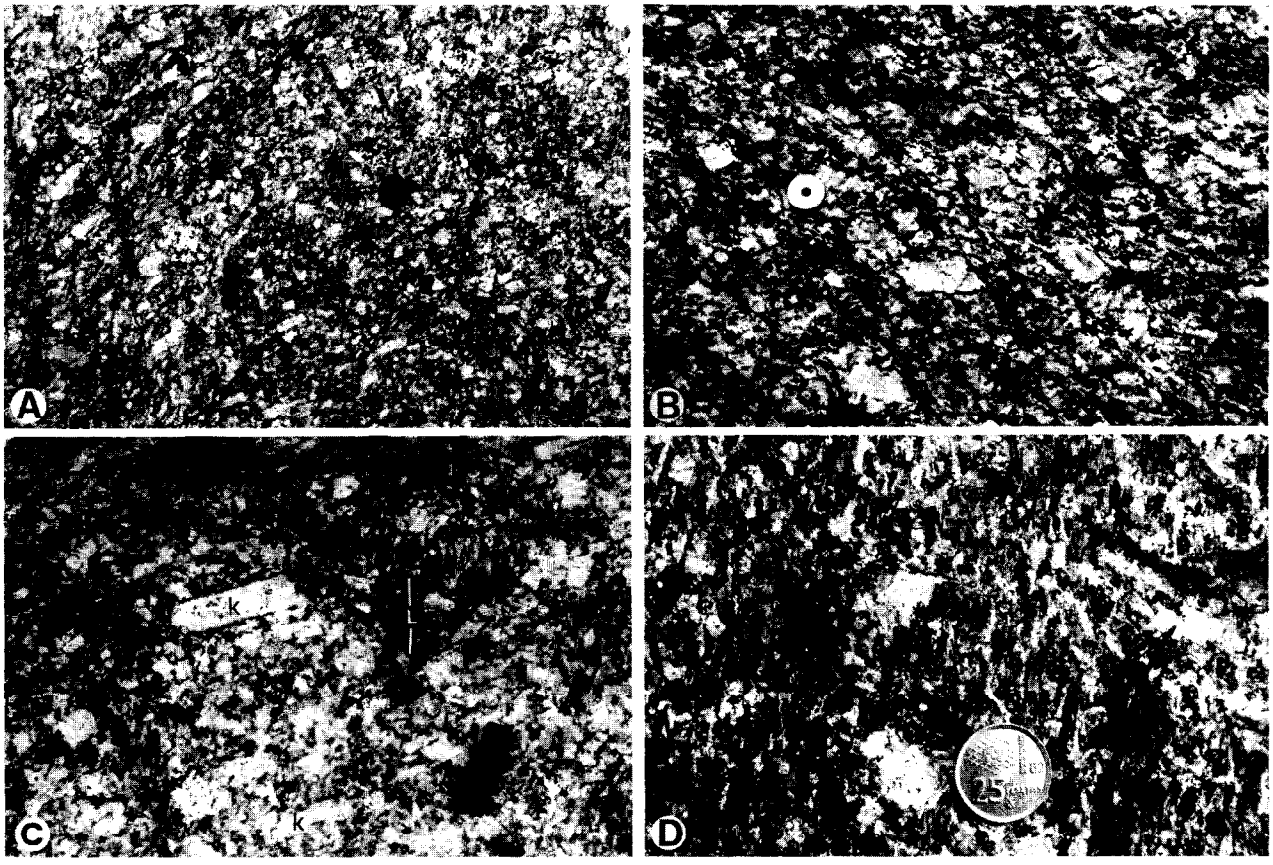

Fig. 2. (A) Magmatic foliation defined by the shape preferred orientation of K-feldspar megacrysts. The diameter of the black hole is 2.5 cm. (B) Highly deformed granodiorite with S-C structures produced by solid state deformation related to the motion of the Chandoiro Fault; coin diameter is 1.8 cm. (C) Weakly deformed granodiorite. Magmatic foliation defined by the preferred orientation of K-feldspar megacryst (K) is partly overprinted by isolated C-planes (black domains) showing a lineation (L) perpendicular to the long axis of K-feldpars. The outcrop section is nearly parallel to the C-planes. (D) Stretching lineation developed on a C-plane. The lineation is defined by the parallel orientation of biotite aggegates with elongated shape. Coin diameter is 2.5 cm.

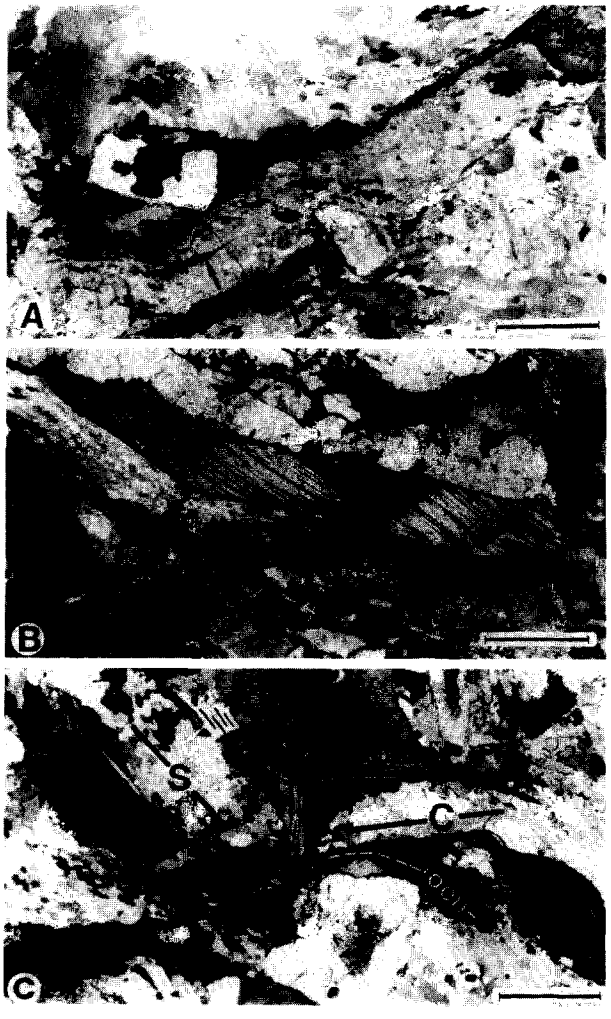

Fig. 3. Microstructures developed on biotite from the S-C mylonites of the Chandoiro Fault: (A) fine-grained biotites concentrate along discrete C-planes whereas S-domains are richer in quartz. Note the presence of biotite fish (black arrows) in the S domains and that the largest C-plane nucleates from a K-feldspar porphyroclast (bar scale: 0.2 mm). (B) Elongated biotite grain from a C-domain, showing the concentration of oxides along the (001)-cleavage and grain boundaries. The (001)-cleavage is parallel to the orientation of C-planes (bar scale: 0.2 mm). (C) Moderately strained granodiorite showing well-developed S- and C-planes, and the progressive reorientation of several biotite grains when approaching the C-plane. Note the lack of preferred orientation of biotite grains (black arrows) in contact with a large K-feldspar. Bar scale: 0.4 mm.

in fine-grained mylonites, and V.9 is a strongly foliated sample from an isolated shear band within moderately strained granodiorites.

Figure 5 summarizes our main results. Most of the analyzed S-C mylonites provide composite magnetic fabrics, where the orientation of the magnetic foliation is between C- and S-planes. In these composite fabrics K_{max} lies close to the stretching lineation (L) whereas K_{int} and the S-C intersection lineation tend to share the same direction (Fig. 5: V.2, V.57, V.60, V.59a). S-C mylonites showing less than 10° between the two sets of planar structures are not included here since they develop new planar structures, the C′ planes, which introduce an additional complication to the interpretation of the composite magnetic fabrics. Our empirical results on the geometrical relationship between the magnetic foliation and field structures do not concur with previous models on the development of composite magnetic fabrics (Borradaile 1988, Housen *et al.* 1993), because such models predict that K_{max} is always parallel to the intersection of the two planar fabrics, whereas we systematically observe that K_{max} tends to be perpendicular to the orientation of the intersection of C- and S-planes.

Some exceptions (represented in Fig. 5 by the stereoplots of samples V.9 and V.59) to the composite magnetic fabrics described here arise as a consequence of the heterogeneity of deformation across the shear zone. V.9, a sample collected in a continuous shear band (in the sense of Burg & Laurent 1978) defined by a sigmoidal mylonitic foliation, does not exhibit C-surfaces. Consequently, its magnetic fabric coincides with the orientation of S-surfaces. Samples V.59a and V.59b illustrate a problem already reported by Borradaile (1988), the influence of domainal fabrics that develop on a local scale and that might not be noticed during sampling. These two samples come from a single core where V.59a, which contains a 2 mm-thick shear band showing a noticeable enrichment in biotite, is isolated in an otherwise undeformed granodiorite forming the whole of V.59b. These shear planes have small dimensions (20–30 cm^2), and strongly resemble biotite schlierens with pencil shapes when intersected by the surface of the frequent granodiorite boulders. Consequently, in this weakly deformed domain of the Veiga granodiorite, the orientation of magnetic fabric ellipsoids is strongly dependent on sampling, and the structural meaning of the AMS fabrics can be easily misinterpreted if they are not complemented by a detailed microstructural study.

PETROFABRIC INTERPRETATION

Petrofabric investigation of sample V.57 (Fig. 6), describes the geometrical relationship between the field structures and the composite magnetic fabrics (the analysis of anisotropy factors is an objective of our ongoing studies).

Magnetic foliation

Modal analysis under the microscope of several XZ-oriented sections of sample V.57 reveals that the S-domains are richer in biotite (69.15% in volume) than the C-domains (30.85%) (Fig. 6B). Therefore, the magnetic foliation should be closer to S than to C. However, given that the magnetic fabric of biotite is essentially controlled by the orientation of its (001)-crystallographic plane, we also have to take into account the preferred crystallographic orientation of biotite within each structural domain. Rose diagrams of biotite (001)-planes show that biotite belonging to C-domains exhibits a stronger crystallographic fabric than biotite belonging to S-domains (Fig. 6C). This reflects the fact that many biotite grains cannot reach the orientation of S-planes, because they are controlled by the orientation of larger K-feldspar porphyroclasts (Fig. 3C). In addition, some isolated biotite grains in S-domains are observed to have rotated towards the orientation of microscopic C-planes which nucleate along the boundaries of large grains of K-feldspar. These observations

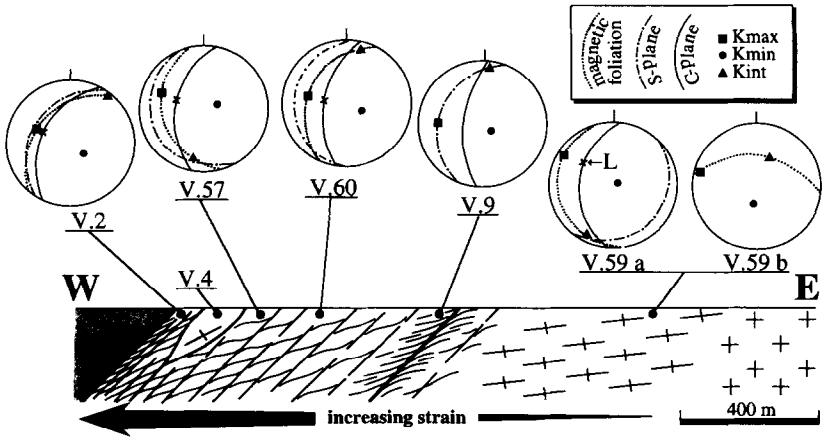

Fig. 5. Schematic cross-section through the Chandoiro Fault, with stereoplots (Wulff nets) of the most representative composite magnetic fabrics and their variation across the shear zone. In the sample V.9 the solid line represents the orientation of a continuous shear band defined by a sigmoidal mylonitic foliation. L represents the orientation of the stretching lineation.

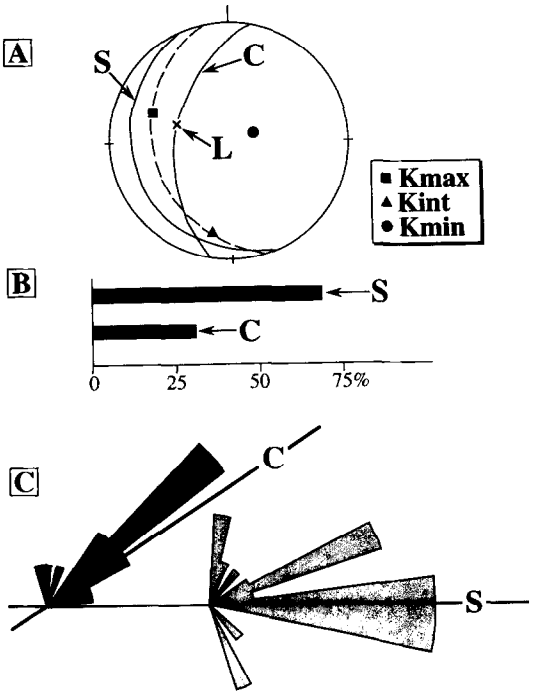

Fig. 6. Composite magnetic fabric of sample V.57; (A) is explained by the balanced effect of two petrofabric factors: the biotite content shown by S- and C-domains (B) and the variation of the preferred crystallographic orientation of biotite (001)-planes (C) in each domain.

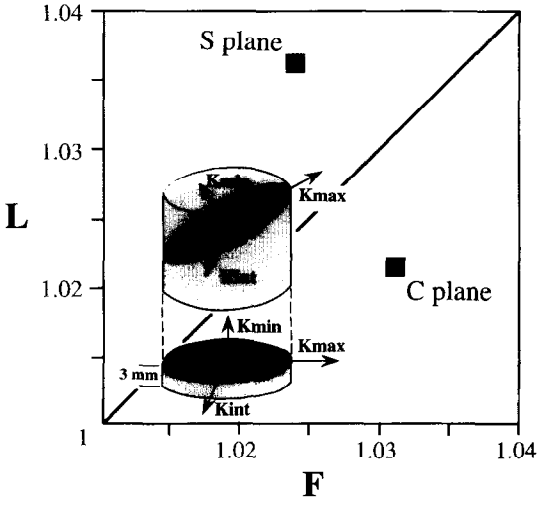

Fig. 7. Representation in a Flinn-type plot, where $F = K_{int}/K_{min}$ and $L = K_{max}/K_{int}$, of the magnetic ellipsoids (black sqares) due to isolated S and C domains from a single drill core. Sketches show the shape of the measured samples and the relationship between the orientation of magnetic fabrics (represented by the principal magnetic axes) and microstructures (S- or C-planes; stretching lineations are indicated by the broken lines) in S- and C-domains. Both magnetic fabrics provide triaxial ellipsoids with K_{max} axes sharing the same trend. These are significant differences with previous analogue and numerical models of composite magnetic fabrics (Housen *et al.* 1993)

suggest that the lower biotite content of C-domains is balanced by a better preferred crystallographic orientation, of this mineral. This explains why, in spite of a pronounced dominance of biotite in the S-domains, the magnetic foliation is farther than expected with respect to the orientation of S-planes.

Magnetic lineation

K_{max} at $\approx 90°$ to the S-C intersection and nearly parallel to the stretching lineation (Fig. 6A) requires an explanation, since magnetic anisotropy studies of slates with composite magnetic fabrics often show that K_{max} is parallel to the bedding–cleavage intersection (Borradaile 1988, Housen *et al.* 1993, Tarling & Hrouda 1993) as do the analogue and numerical models of Housen *et al.* (1993). The widespread presence of brown biotite on S- and C-planes together with the constant assymmetry of structures across the Chandoiro fault, suggest that S- and C-planes are coeval structures that were formed during a single deformation event dominated by simple shear. This is an important difference with the slates, where the two planar structures (bedding and cleavage) reflect completely separate processes, hence their respective shape anisotropies are not related to each other. The analogue and numerical models of composite magnetic fabrics performed by Housen *et al.* (1993) result from the combined effect of individual component fabrics perfectly uniaxial-oblate, with $K_{max} = K_{int} > K_{min}$. However, in the studied S-C granitic mylonites both structures, the S- and C- planes, present triaxial magnetic ellipsoids ($K_{max} > K_{int} > K_{min}$) of prolate type in S-domains and of oblate shape in C-domains (Fig. 7). In addition, K_{max} axes have different plunges but share the same trend (Fig. 7). These significant differences with the model conditions (Housen *et al.* 1993) could explain why, in S-C mylonites, the magnetic lineation remains at 90° of the intersection between the two planar fabrics.

These observations are consistent with the deformation process responsible for the development of S-C mylonites because, due to the imposition of a common flow kinematics, the deformation of biotite by intracrystalline slip on (001)-planes leads to the growth of biotite aggregates, on both the S- and C-domains, strongly elongated parallel to the shear direction. Consequently, the magnetic fabric of these S-C mylonites reflects the additive effect of two planar structures with shape anisotropies sharing a common elongation strike.

Acknowledgements—Financial support from the UPV research Credit 121.310-EB 182/92 and DGCICYT PB93-1149-C03-03 is gratefully acknowledged. D. Whitelam is thanked for English revision. J. L. Bouchez is also acknowledged for suggesting significant improvements to this paper.

REFERENCES

Benn, K. 1994. Overprinting of magnetic fabrics in granites by small strains: numerical modelling. *Tectonophysics* **233**, 153–162.

Berthé, D., Choukroune, P. & Jegouzo, P. 1979. Orthogneiss, mylonite and non coaxial deformation of granites: the example of the South Armorican Shear Zone. *J. Struct. Geol.* **1**, 31–42.

Borradaile, G. H. 1988. Magnetic susceptibility, petrofabrics and strain. *Tectonophysics* **156**, 1–20.

Borradaile, G. J. 1991. Correlation of strain with anisotropy of magnetic susceptibility (AMS). *Pure Appl. Geophys.* **135**, 15–29.

Borradaile, G. J. & Alford, C. 1988. Experimental shear zones and magnetic fabrics. *J. Struct. Geol.* **10**, 895–904.

Bouchez, J. L., Gleizes, G., Djouadi, T. & Rochette, P. 1990. Microstructure and magnetic susceptibility applied to emplacement kinematics of granites: the example of the Foix pluton (French Pyrenees). *Tectonophysics* **184**, 157–171.

Burg, J. P. & Laurent, Ph. 1978. Strain analysis of a shear zone in a granodiorite. *Tectonophysics* **47**, 15–42.

Graham, J. W. 1954. Magnetic susceptibility anisotropy, an unexploited petrofabric element. *Bull. geol. Soc. Am.* **65**, 1257–1258.

Housen, B. A., Richter, C., Van der Pluijm, B. 1993. Composite magnetic anisotropy fabrics: experiments, numerical models, and implications for the quantification of rock fabrics. *Tectonophysics* **220**, 1–12.

Hrouda, F. 1986. The effect of quartz on the magnetic anisotropy of quartzites. *Studia Geophysica et Geodetica* **30**, 39–45.

Hrouda, F. 1991. Models of magnetic anisotropy variations in sedimentary thrust sheets. *Tectonophysics* **185**, 203-210.

Hrouda, F. 1993. Theoretical models of magnetic anisotropy to strain relationship revisited. *Phys. Earth Planet. Interiors* **77**, 237–249.

Iglesias, M. & Choukroune, P. 1980. Shear zones in the Iberian Arc. *J. Struct. Geol.* **2**, 63–68.

Iglesias, M. & Varea, R. 1982. *Memoria y Hoja n°* 228 (Viana del Bollo). Mapa geológico de España. E 1:50000, IGME, Madrid.

Jelinek, , V. 1981. Characteristics of the magnetic fabric of rocks.. *Tectonophysics* **79**, 163–167.

Jover, O., Rochette, P., Lorand, J.P., Maeder, M. & Bouchez, J.L. 1989. Magnetic mineralogy of some granites from the French Massif Central: origin of their low-field susceptibility. *Phys. Earth Planet. Interiors* **55**, 79–92.

Kligfield, R., Owens, W. H. & Lowrie, W. 1981 Magnetic susceptibility anisotropy, strain and progressive deformation in Permian sediments from the Maritime Alps (France). *Earth Planet. Sci. Lett.* **55**, 181–189.

Lister, G. S. & Snoke, A. W. 1984. S-C mylonites. *J. Struct. Geol.* **6**, 617–638.

Potter, D. K. & Stephenson, A. 1988. Single-domain particles in rocks and magnetic fabric analysis. *Geophys. Res. Lett.* **15**, 1097–1100.

Rochette, P. 1987. Magnetic susceptibility of the rock matrix related to magnetic fabric studies. *J. Struct. Geol.* **9**, 1015–1020.

Rochette, P. & Vialon, P. 1984. Development of planar and linear fabrics in Dauphinois shales and slates (French Alps) studied by magnetic anisotropy and its mineralogical control. *J. Struct. Geol.* **6**, 33–38.

Rochette, P., Scaillet, B., Guillot, S., Le Fort, P. & Pecher, A. 1994. Magnetic properties of the High Himalayan leucogranites: Structural implications. *Earth Planet. Sci. Lett.* **126**, 217–234.

Román-Berdiel, T., Pueyo-Morer, R. & Casas-Sainz, A. 1995. Granite emplacement during contemporary shortening and normal faulting: structural and magnetic study of the Veiga massif (NW Spain). *J. Struct. Geol.* **17**, 1689–1706.

Tarling, D. H. & Hrouda, F. 1993. In: *The magnetic anisotropy of rocks*. Chapman and Hall, London, 217 pp.

Van der Voo, R. & Klootwijk, C. T. 1972. Paleomagnetic reconnaissance study of the Flamanville granite with special reference to the anisotropy of its susceptibility. *Geologie Mijnb.* **51**, 609–617.